

This is the accepted manuscript made available via CHORUS. The article has been published as:

Impeding Hohlraum Plasma Stagnation in Inertial-Confinement Fusion

C. K. Li, F. H. Séguin, J. A. Frenje, M. J. Rosenberg, H. G. Rinderknecht, A. B. Zylstra, R. D. Petrasso, P. A. Amendt, O. L. Landen, A. J. Mackinnon, R. P. J. Town, S. C. Wilks, R. Betti, D. Meyerhofer, J. M. Soures, J. Hund, J. D. Kilkenny, and A. Nikroo

Phys. Rev. Lett. **108**, 025001 — Published 11 January 2012

DOI: [10.1103/PhysRevLett.108.025001](https://doi.org/10.1103/PhysRevLett.108.025001)

Impeding Hohlraum Plasma Stagnation in Inertial-Confinement Fusion

C. K. Li^{1*}, F. H. Séguin¹, J. A. Frenje¹, M. J. Rosenberg¹, H. G. Rinderknecht¹, A. B. Zylstra¹,
R. D. Petrasso¹, P. A. Amendt², O. L. Landen², A. J. Mackinnon², R. P. J. Town², S. C. Wilks²,
R. Betti^{3,†}, D. D. Meyerhofer^{3,†}, J. M. Soures³, J. Hund⁴, J. D. Kilkenny⁴ and A. Nikroo⁴

¹*Plasma Science and Fusion Center, Massachusetts Institute of Technology,
Cambridge, Massachusetts 02139, USA*

²*Lawrence Livermore National Laboratory, Livermore, California 94550 USA*

³*Laboratory for Laser Energetics, University of Rochester, Rochester, New York 14623, USA*

⁴*General Atomics, San Diego, California, 92186 US*

This Letter reports the first time-gated proton radiography of the spatial structure and temporal evolution of how the fill gas compresses the wall blow-off, inhibits plasma jet formation, and impedes plasma stagnation in the hohlraum interior. The potential roles of spontaneously generated electric and magnetic fields in the hohlraum dynamics and capsule implosion are discussed. It is shown that interpenetration of the two materials could result from the classical Rayleigh-Taylor instability occurring as the lighter, decelerating ionized fill gas pushes against the heavier, expanding gold wall blow-off. This experiment showed new observations of the effects of the fill gas on x-ray driven implosions, and an improved understanding of these results could impact the ongoing ignition experiments at the National Ignition Facility.

PACS numbers: 52.38.Fz, 52.30.-q, 52.57.-z, 52.50.Jm

The symmetry requirements for achieving ignition are fundamental and impose strict constraints in inertial-confinement fusion (ICF) [1-7]. The tolerable drive asymmetry of an implosion, in a time-integrated sense, is less than 1-2% and depends on the ignition margin [3,4]. In the indirect-drive approach to ICF, low-mode-number implosion asymmetries are a major concern because the quasi-uniform hohlraum radiation field provides drive with minimal high-

mode-number non-uniformities [3-8]. An example of such an asymmetry would be a time integrated P2 (2nd-order Legendre Polynomial) non-uniformity that could lead to different radial velocities and densities at pole and equator, converting less kinetic energy into the internal energy and resulting in a higher drive energy required for ignition.

The high-Z plasma from the wall blow-off [usually gold (Au) or uranium], which causes motion of the laser absorption region and alters the spatial distributions of x-ray energy sources and sinks, has been shown to cause low-mode-number implosion asymmetries [3-8]. The blow-off quickly fills the interior of an initially empty (optically thin) hohlraum, leading to early on-axis plasma stagnation [3-8]. The stagnated plasma has high pressure and can asymmetrically compress the capsule.

To achieve required drive symmetry, the motion of the laser-deposition (x-ray emission) region must be minimized. Two approaches that have been proposed are to over-coat a hohlraum wall surface with low-Z liner and to fill a hohlraum interior with low-Z gas [4]. Neither the liner nor the fill gas stops the wall blow-off, but they displace the low-density plasmas. In the first approach, plasma jets are formed due to the interaction of pairs of adjacent, expanding plumes of low-Z liner blow-off [4,9]. The radially moving jets are supersonic and quickly stagnate at the hohlraum interior, resulting in asymmetries in both drive and the capsule implosion. The ignition campaign at the National Ignition Facility (NIF) currently adopts the second approach [3-7]. Hohlräume are filled with helium-4 gas [6] at a pressure ~ 0.4 atm (when fully ionized, $n_e \sim 0.04 n_{crit.}$, the critical electron density for 0.35- μm laser light). The gas is contained with thin polyimide windows over the laser entrance holes (LEHs).

This Letter presents the first proton radiography observations of the effects of gas fill on impeding the hohlraum plasma stagnation. The experiments, illustrated schematically in Fig.1a, were performed at the OMEGA Laser Facility [10]. Radiographic images were made with 15-

MeV protons at various implosion times through the LEH [9,11]. Figure 1 shows two different types of images: proton fluence versus position (Fig. 1b) and proton mean energy versus position (Fig. 1c). The proton fluence piles up in the gaps between the two expanding plasma plumes and in the region between the imploding capsule and the expanding plasmas, forming a 5-prong, asterisk-like pattern [8] that is a consequence of the OMEGA laser beam distribution [9,11]. Contrary to earlier experiments that showed a deficit in proton fluence in these regions for vacuum hohlraums [9,11], this fluence surplus suggests that no high-density plasma jets were formed. The fill gas along the laser beam path is fully ionized. The interfaces between the gas plasma and the Au wall blow-off are constrained near the wall surface (Fig. 1b, indicated by the open arrows). Figure 2 shows the measured Au-wall plasma-fill gas interface radius as a function of time compared with the sound speed [$C_s \propto (ZT_e m_i^{-1})^{1/2}$] that sets the scale for hydrodynamic rarefaction expansion in vacuum [11,12]. The expansion speed of the Au blow-off is estimated to be $\sim (2.1 \pm 0.3) \times 10^7 \text{ cm s}^{-1}$, which is slower than $C_s \sim 2.5 \times 10^7 \text{ cm s}^{-1}$, indicating that the wall blow-off expansion has been compressed by the fill gas [13,14]. These measurements show that the fill gas impedes the wall plasma expansion.

An additional interface appears in the region around the imploding capsule (1.65 ns, Fig. 1b). It is identified as the interface between the capsule CH ablation and the fill gas plasma. Because the implosion is nearing the deceleration phase, with the typical implosion velocity, $v_{\text{imp}} [\propto I_{15}^{1/8} \ln(m_0/m)] \sim 2\text{-}3 \times 10^7 \text{ cm s}^{-1}$ and velocity of outward-moving ablated capsule material $v_{\text{abl}} [\propto I_{15}^{9/40}]$, where I_{15} is the laser intensity in units of 10^{15} W/cm^2 $\sim C_s$, the capsule is expected to be essentially unaffected by the pressure generated in this region [4].

While the proton fluence shows large variations (Fig. 1b), the proton energy shows less variation (Fig. 1c) until later times (1.65 ns). This suggests that the trajectories of these backlighting protons have been largely affected by fields around the capsule and not by proton

scattering in the plasma, because Coulomb interactions are always accompanied by energy loss [9,15].

To explore the mechanism for forming such a unique spatial (fluence) structure and its effects on impeding the hohlraum wall plasma expansion and drive dynamics, experiments were performed with solid, spherical CH targets driven in both gas-filled Au hohlraums and CH-lined vacuum Au hohlraums (Fig. 3). The two images show related asterisk-like structures (with spokes in the gaps between pairs of expanding plasma plumes) but with opposite proton fluence distributions: protons were focused into the gaps (high-fluence spokes) for the gas-filled hohlraum (Fig. 3a) but were deflected away from the spokes in the CH-lined vacuum hohlraum (Fig. 3b). The role of a spontaneously generated magnetic (B) field in these interactions can be excluded by symmetry since the toroidal B -field topology around the laser spots [16,17] cannot result in such azimuthal proton deflections [9]. Lateral electric (E) fields [17,18] associated with azimuthally oriented electron pressure gradients (∇P_e) in the plasma plumes and in the radial plasma jets, $E = -\nabla P_e / en_e$, may be the source of these deflections. Another physical mechanism that could explain the deflection near the capsule before 0.5 ns is the E field associated with a supersonic heat front generated by the laser-heated gas channels that are in close proximity to the capsule. Work is in progress to quantitatively assess the relative importance of this mechanism in the generation of such a field. Since Figs. 3a and 3b show opposite deflections, E must have pointed in opposite directions.

As illustrated in the cartoon in Fig. 3a for the gas-filled hohlraum, the possible high plasma pressure should have resulted from an increase of temperature inside the plasma plume and ionized gas that was observed in earlier NOVA experiments [8] and confirmed by numerical simulation [8, 19]. The steep ∇P_e results in strong E fields that point laterally away from the plumes, deflecting the backlighting protons into the gaps between pairs of approaching plasma

plumes. For these underdense gas plasmas ($\sim 0.04 n_{crit}$), the rapidly rising plasma temperature in the region where the laser passes does not result from continuous laser heating but is a consequence of the inhibition of heat flow due to the self-generated megaGauss B field [8,9,11], because the electron thermal transport is reduced by a factor of $(1+\omega_{ce}^2 \tau^2)^{-1}$, where ω_{ce} is the electron gyro frequency and τ is the collision time [17,18]. Including the contribution from magnetized window plasma, the Hall parameter $\omega_{ce} \tau$ is ~ 10 (ref. 8). Eventually, the combination of inverse bremsstrahlung absorption in Au wall and electron conduction establishes a near equilibrium plasma conditions in the laser propagation channel, and the quasi pressure balance leads to continuous plasma heating and temperature increase [4].

The behavior and dynamics are different in the laser-irradiated CH-lined, Au vacuum hohlraum (Fig. 3b). Although the ablated CH wall helps to compress the Au blow-off, radially moving CH plasma jets are generated with the Au blow-off trailing [9]. This process is initiated by the CH liner ablating from the wall, which subsequently expands with the continual arrival of wall blow-off into the region between the two adjacent expanding plumes. These plasmas collide with one another, leading to the formation of the dense plasma spokes that are redirected radially and move towards the hohlraum interior. The steep ∇P_e around the jets results in radial E fields that deflect the imaging protons away from the jets and leads to the asterisk-like spoke structure in the fluence images (Fig. 3b). The inward jets travel with supersonic speed ($\sim 4C_s$) generating an early-time stagnation pressure that affects capsule implosion symmetry and dynamics [9], a phenomenon also observed in the pure vacuum Au hohlraum-driven experiments [11].

The widths of the spokes in the image of vacuum hohlraum (Fig.3b) can be used with the imaging geometry to estimate the field $\int E \times d\ell \sim 3 \times 10^5$ V (where $d\ell$ is the differential path length

along the proton trajectory through the field area) [9]. A scale length of ~ 0.1 cm (\sim laser spot width) for the field in a jet spoke implies $E \sim 3 \times 10^6$ V cm $^{-1}$.

To further study the dynamics of the interface and its effect on impeding the plasma stagnation, capsule implosions were performed with a denser hohlraum gas fill (~ 1 atm, C₅H₁₂) at two sampling times (Fig. 4). A relatively smooth interface appears between the expanding wall blow-off and the ionized fill gas at 0.8 ns, while chaotic spatial structure and interface interpenetration are evident at 1.6 ns. This interpenetration could be caused by hydrodynamic instabilities. The surface perturbations that are seeded at the plume front can be amplified by the classical Rayleigh-Taylor (RT) instability occurring at the interface of the lighter, decelerating, ionized gas plasma and the heavier, expanding Au blow-off [4]. This instability has a growth rate [4] $\gamma_{RT} \approx (2\pi A_t a k)^{1/2}$, where a is the acceleration, $\sim 10^{16}$ cm s $^{-2}$ estimated from Fig. 1b; $k = m(2\pi r)^{-1}$ is the perturbation wave number. As an example, for a mode number $m \sim 50$ at half the hohlraum radius $r \sim 0.5 \times 0.12$ cm, $k \sim 130$ cm $^{-1}$; and $A_t = (\rho_2 - \rho_1) / (\rho_2 + \rho_1)$ is the Atwood number at the interface. For $\sim 0.1 n_{crit}$ the gas fill plasma has $\rho_1 \approx 3$ mg cm $^{-3}$ while the Au plasma has a $\rho_2 \approx 10$ mg cm $^{-3}$; thus $A_t \approx 0.54$. A rough estimate gives $\gamma_{RT} \sim 2.7 \times 10^9$ s $^{-1}$ and a perturbation grows by a factor of ~ 15 in a period of 1 ns. A similar interaction process occurred between the ablated capsule plasma and the gas plasma. This effect could reduce the benefit of the gas fill because the enhanced interpenetration (or mixing) between the Au blow-off and the gas plasma could lead to high-Z material stagnating earlier in the hohlraum interior. This effect does not appear to be severe because it happens during the coasting phase when the capsule implosion moves at a speed, v_{imp} , that is comparable to, or even faster than, the outward ablation speed ($\sim C_s$). At this time the high-Z blow-off should be sonically decoupled from the imploding capsule.

In summary, we have performed the first time-gated proton radiography of the spatial structure and temporal evolution of how the fill gas compresses the wall blow-off, inhibits plasma jet formation, and impedes plasma stagnation in the hohlraum interior. The potential roles of spontaneously generated electric and magnetic fields in the hohlraum dynamics and capsule implosion have been discussed. We have shown that the plasma interpenetration could result from the classical Rayleigh-Taylor instabilities occurring as the lighter, decelerating ionized fill gas pushes against the heavier, expanding gold wall blow-off. This experiment showed new observations of the effects of the fill gas on x-ray driven implosions, and an improved understanding of these results could impact the ongoing ignition experiments at the NIF.

This work was supported in part by US DOE and LLE National Laser User's Facility (DE-FG52-07NA28059 and DE-FG03-03SF22691), LLNL (B543881 and LDRD-08-ER-062), LLE (414090-G), FSC (412761-G), and General Atomics (DE-AC52-06NA 27279). A. B. Zylstra is supported by the Stewardship Science Graduate Fellowship (DE-FC52-08NA28752).

* ckli@mit.edu

[†] Also at Department of Mechanical Engineering, and Physics and Astronomy, University of Rochester.

- [1] J. Nuckolls *et al.*, *Nature* **239**, 139 (1972).
- [2] R. L. McCrory *et al.*, *Nature* **335**, 225 (1989).
- [3] S. W. Haan *et al.*, *Phys. Plasmas* **2**, 2480 (1995).
- [4] J. D. Lindl, *Inertial Confinement Fusion* (Springer, NY 1999).

- [5] S. Atzeni and J. Meyer-Ter-Vehn, *The Physics of Inertial Fusion* (Clarendon, Oxford, 2004).
- [6] S. H. Glenzer *et al.*, *Science* **327**, 1228 (2010).
- [7] O. L. Landen *et al.*, *Phys. Plasmas* **17**, 056301 (2010).
- [8] S. H. Glenzer *et al.*, *Phys. Plasmas* **6**, 2117 (1999). N. D. Delamater *et al.*, *AIP Conf. Proc.* **369**, 95 (1996).
- [9] C. K. Li *et al.*, *Science* **327**, 1231 (2010).
- [10] J. M. Soures *et al.*, *Phys. Plasmas* **3**, 2108 (1996).
- [11] C. K. Li *et al.*, *Phys. Rev. Lett.* **102**, 205001 (2009).
- [12] R. P. Drake, *High-energy-density physics* (Springer, NY 2006).
- [13] For an adiabatic rarefaction expansion of an ideal gas, the expansion speed is $3C_s$ in vacuum, while the hot electrons advancing ahead of the rarefaction expansion due to their high mobility may further boost the motion of leading edge CH and Au ions ablating off the hohlraum wall by an additional C_s factor [9].
- [14] The similar gas-wall blowoff interface movement have been previously measured using x rays by T. J. Orzechowski *et al.*, *AIP Conf. Proc.* **369**, 125 (1996); E. L. Dewald, *et al.*, *IFSA 2003*, 490 (2004); and T. E. Tierney *et al.*, *Proc. SPIE* **6261**, 626106 (2006);
- [15] C. K. Li *et al.*, *Phys. Rev. Lett.* **70**, 3029 (1993).
- [16] R. D. Petrasso *et al.*, *Phys. Rev. Lett.* **103**, 085001 (2009).
- [17] S. I. Braginskii, *Review of Plasma Physics* 1 (Consultants Bureau, New York, 1965).
- [18] M. G. Haines, *Phys. Rev. Lett.* **78**, 254 (1997).
- [19] Such a temperature rise has been seen with Thomson scattering in NOVA experiments, where the electron temperature ~ 2 keV was measured on the axis of a gas-filled hohlraum at early times during a 1-ns laser pulse ($I \approx 10^{15}$ W cm⁻²), and in LASNEX simulations of the development of hot regions along the laser pass channels [8].

- [20] A. Nishiguchi *et al.*, *Phys. Rev. Lett.* **53**, 262 (1984).
 [21] C. K. Li *et al.*, *Phys. Rev. Lett.* **97**, 135003 (2006).
 [22] D. D. Meyerhofer *et al.*, *Phys. Plasmas* **8**, 2251 (2001).
 [23] C. K. Li *et al.*, *Phys. Rev. Lett.* **100**, 225001 (2008).
 [24] P. A. Amendt *et al.*, *Plas. Phys. Contr. Fus.* **51**, 124048 (2009).

FIGURE CAPTION:

FIG. 1. (Color) (a) Experimental setup. The two photos show an Au hohlraum filled with ~ 0.4 -atm neopentane gas (C_5H_{12}) and containing a CH capsule (30- μ m-thick plastic shell of diameter 550 μ m, either empty or filled with 50 atm H_2 gas). A proton backlighter (imploded D^3He -filled thin-glass-shell capsule driven by 30-OMEGA laser beams [21]) is typically 1 cm from the hohlraum center and has the illustrated monoenergetic spectra from the reactions $D+^3He \rightarrow \alpha+p$ (14.7MeV) and $D+D \rightarrow T+p$ (3.0MeV), recorded with CR39 detector (27 cm from the hohlraum center). The hohlraums had 30- μ m-thick gold walls, 100% LEH, 2.4-mm diameter, and 3.8-mm length. The hohlraum was driven by 30 laser beams with a wavelength of 0.351 μ m and total laser energy ~ 11 kJ in a 1-ns square pulse. The laser beams had full spatial and temporal smoothing [22]. Radiographic images of proton fluence (b) and energy (c) taken with 15-MeV D^3He protons (the particle energy are slightly upshifted from their birth energy due to the capsule positive charging) at various implosion times. Within each image, darker means higher proton fluence (b) or lower proton energy (c). The open arrows in (b) point to the interfaces between the Au wall blow-off and gas plasmas. For the image at 1.65 ns, the solid arrow points to the interface between the capsule ablator and gas plasma.

FIG. 2. (Color) Measured interfaces between the Au wall blow-off and the gas plasma (open diamonds), and between the capsule and the gas plasma (solid squares), are compared to motion at multiples of the sound speed. The uncertainties for sampling times were ~ 90 ps (the backlighter burn duration) while for the radius they were $\sim 10\%$ (the variation in image circularity). Linear fit yields the expansion speed $v \approx (2.1 \pm 0.3) \times 10^7$ cm s $^{-1}$ (reduced $\chi^2 = 0.662$)

FIG. 3. (Color) The proton fluence distributions are showing surplus in the regions between the pairs of expanding plasma plumes in a gas-filled, Au hohlraum (a) but showing deficit in a CH-lined, vacuum Au hohlraum (b), indicating opposing directions of the self-generated electric fields as illustrated schematically by the corresponding cartoons.

FIG. 4 (Color online) (a) Proton fluence images of capsule implosions driven by gas-filled hohlraums. The open arrows point to interfaces between Au wall blow-off and gas plasma. A relatively smooth interface appears between the expanding wall blow-off and the ionized fill gas at time 0.8 ns, while chaotic spatial structure and interface interpenetration are evident at time 1.6 ns. The fluence surplus inside the imploding capsule (0.8 ns) resulted from self-generated radial E fields [23,24]. Proton energy images given in (b) indicate that the energy around interfaces are relative uniform compared with the surrounding background, suggesting the energy loss are very small and are therefore negligible.

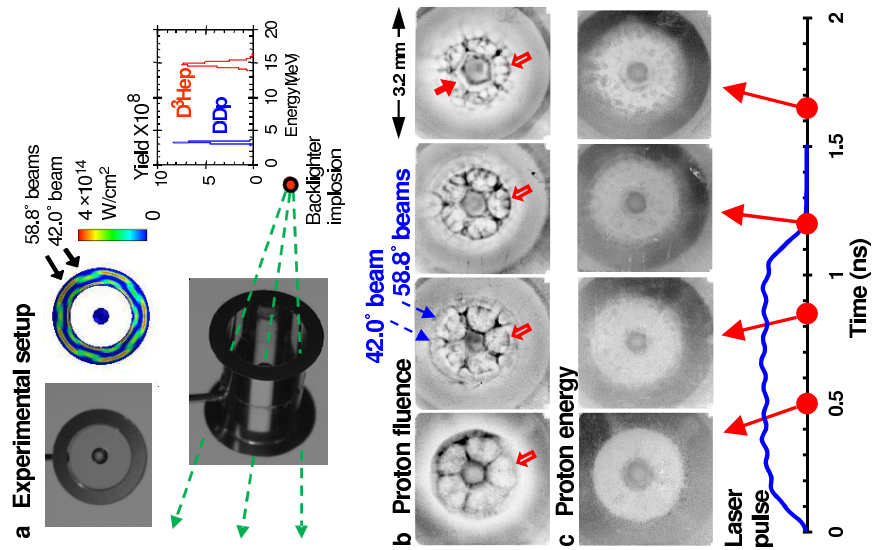


Figure 1

LZ12097 21NOV2011

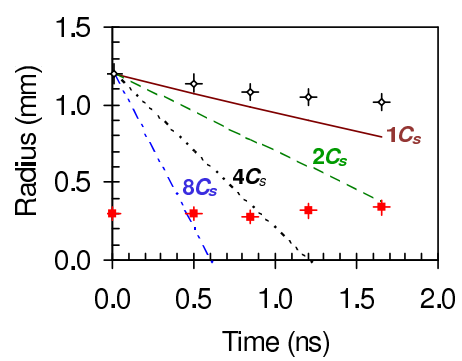


Figure 2 LZ12097 21NOV2011

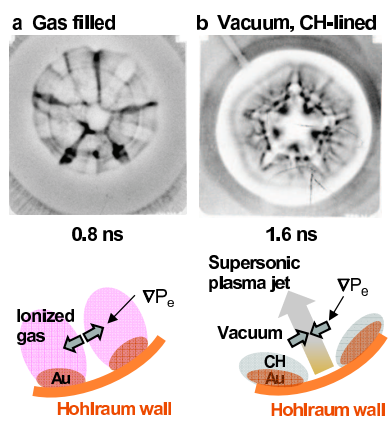


Figure 3 LZ12097 21NOV2011

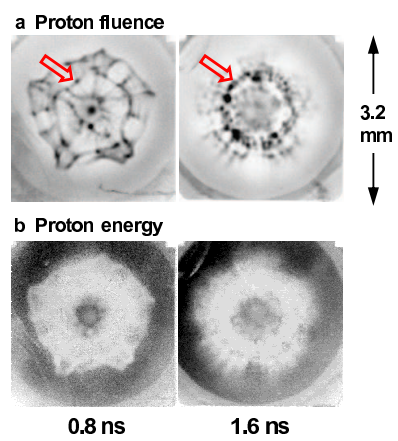


Figure 4

LZ12097

21NOV2011